Environmental Science: Atmospheres

ROYAL SOCIETY OF CHEMISTRY

PAPER

View Article Online
View Journal | View Issue

Cite this: *Environ. Sci.: Atmos.*, 2026, **6**, 703

Identifying the sources of nucleation mode particles by analyzing black carbon coating thickness in urban atmospheres

Hong Zhang,†[abc] Jun Liu,†[a] Yonghong Wang,*[a] Quan Liu,[d] Tianzeng Chen,[a] Peng Zhang,[a] Qingxin Ma[a] and Biwu Chu[a]

Nucleation mode particles (NMPs, less than 25 nm in diameter) are ubiquitous in the atmosphere and have a negative impact on human health and climate. New particle formation (NPF) from extremely low volatile vapors is the dominating source of NMPs globally, but direct emissions from on-road vehicles are also an important source in the urban boundary layer. However, quantifying the contribution of NMPs in the urban boundary layer from NPF and direct emissions is a challenge owing to the complex sourcing and evaluation processes of NMPs. Here, black carbon coating thickness, together with the quantity of a fingerprint organic aerosol marker related to on-road vehicle emissions (HOA, hydrocarbon-like organic aerosol), was utilized to distinguish and determine the two main sources of NMPs. Owing to the constrains of this approach, the influence of upward wind on NMP transportation was excluded. Statistical analysis showed that NPF was the dominant source of NMPs under NPF, non-NPF, and haze conditions, whereas direct vehicle emissions remained a relatively constant contributor.

Received 4th February 2026
Accepted 16th March 2026

DOI: 10.1039/d6ea00021e

rsc.li/esatmospheres

Environmental significance

The nucleation mode particles (NMPs, less than 25 nm in diameter) are ubiquitous in the atmosphere and have negative impacts on the human health and climate. Both new particle formation and vehicle emissions can contribute to the formation of NMPs; however, quantifying the contributions of NPF and direct emissions on NMP formation in urban atmospheres is challenging owing to the complex sourcing and evaluation processes of NMPs. In this work, black carbon coating thickness and a fingerprint organic aerosol marker related with on-road vehicle emissions (HOA, hydrocarbon-like organic aerosol) were first utilized to distinguish and determine the two main sources of NMPs. Using this approach, the influence of transport from upwind regions on NMPs was excluded, and the distribution of NMP number concentrations in fresh local air masses was finally obtained.

Introduction

Atmospheric nucleation mode particles (NMPs) are usually defined as particulate matter of less than 25 nm in diameter. NMPs are the smallest aerosol particles, which are formed from atmospheric clusters or emitted from combustion sources. Globally, atmospheric NMPs are mainly formed from the oxidation of gas vapors and subsequent gas-to-particle conversion,[1–3] which is called new particle formation (NPF), and they have a remarkable influence on the global climate.[4,5] In the urban boundary layer, on-road vehicle emissions are an important source of atmospheric NMPs,[6–8] which have adverse effects on human health.[9,10] Recent investigations reveal that the formation of NMPs is highly related to haze episodes as they result in the emergence of most of the seed aerosols, which aggravates haze pollution.[11]

Owing to the significant role of NMPs in causing haze pollution, the contribution of NPF and vehicle emissions to the formation of NMPs in urban atmospheres has been subjected to intensive investigations.[12] Rönkkö *et al.*[12] found that nanoparticles (1.3–3 nm) emitted from motor vehicles represent 20–54% of the total NMP concentration in ambient air.[8] In addition, field observations show that sulfuric acid-derived NPF contributes significantly to the formation of NMPs in urban atmospheres.[13–16] Moreover, the growth of these NMPs are governed by the condensation of oxygenated organic molecules (OOMs) that are formed from the oxidation of anthropogenic and biogenic volatile organic compounds (VOCs).[17,18]

Although NPF and on-road vehicle emissions have been acknowledged as the most important sources of nanoparticles

[a]*Laboratory of Atmospheric Environment and Pollution Control, Research Center for Eco-Environmental Sciences, Chinese Academy of Sciences, Beijing 100085, China. E-mail: yonghongwang@rcees.ac.cn*

[b]*Nanjing Climblue Technology Co. Ltd, Nanjing 211135, China*

[c]*Beijing Key Lab for Source Control Technology of Water Pollution, College of Environmental Science and Engineering, Beijing Forestry University, Beijing 100083, China*

[d]*State Key Laboratory of Severe Weather & Key Laboratory of Atmospheric Chemistry of CMA, Chinese Academy of Meteorological Sciences, Beijing 100081, China*

† Hong Zhang and Jun Liu contributed equally to this work.

in the urban atmosphere, there is no appropriate way to effectively distinguish their respective contributions. The NMP concentrations measured at a site reflect the combined effects of transport from upwind regions, local traffic emissions, and local NPF. In addition, NMPs are subjected to coagulation with larger particles during atmospheric processes.[19,20] Hydrocarbon organic aerosol (HOA) is a type of organic aerosol specifically emitted by on-road vehicles due to incomplete combustion. The elemental composition of HOA mainly consists of hydrogen and carbon, and HOA can be rationally resolved as a separate factor by PMF from fragment ions measured by HR-ToF-AMS.[21] The emission from on-road vehicles is an important source of black carbon (BC) aerosol.[22,23] During the atmospheric transport process, BC will be aged due to the interaction between BC and vapors.[24] Consequently, the aging degree of BC can be retrieved from the measurements of particle coating thickness by a single particle soot photometer (SP2).[25] With the long-range transport of air masses, the diameter ratio of the particle to its soot core (Dp/Dc) is elevated owing to aging and coating on the surface. However, when the particles are from fresh local sources of direct emissions and NPF, the ratios of Dp/Dc are low.

In this study, we conducted an intensive filed campaign in downtown Beijing in the autumn of 2021. We used two scanning mobility particle sizers (SMPS, TSI, USA) to measure ambient particles from 5–700 nm, ensuring that the measurement range included NMPs. A novel approach using the ratio of black carbon coating thickness to infer the NMP source is proposed. In this new method, the interference from the transport of air mass was rationally removed and the contributions of NPF and vehicle emissions to observed NMPs in urban areas were evaluated under different pollution scenarios.

Materials and methods

Site description

The monitoring site, the Research Center for Eco-Environmental Sciences, Chinese Academy of Sciences, is located in Haidian District, Beijing (40.03° N, 116.24° E, 52 m above the mean sea level). This site is surrounded with Beijing–Tibet Expressway to the northeast, Beijing–Xinjiang Expressway to the northwest and other urban arterial roads. There are no significant industrial emissions in the area. The experiments were carried out from October 2 to November 6, 2021, with the average daytime temperature and relative humidity (RH) in this monitoring site being 13.8 °C and 41.2% compared with 9.6 °C and 57.2% at night. There were also occasional rainfall and fog conditions prevailed over the target region.

Measurements and instruments

The concentration and size distribution of particles (from 5 nm to 700 nm) were measured using two scanning mobility particle sizers (SMPS, TSI, USA). One system comprised a differential mobility analyzer (DMA, 3081, TSI, USA) and a condensation particle counter (CPC, 3775, TSI, USA), while the other comprised a DMA (3072, TSI, USA) and a CPC (3776, TSI, USA). A single particle soot photometer (SP_2, Droplet Measurement Technologies, Inc., Boulder, CO, USA) was used to determine the size distribution and mixing state of the BC particles in the atmosphere. The operating principle of SP_2 can be found in other studies.[26,27] In a nutshell, SP_2 uses a high-intensity laser beam (wavelength $\lambda = 1064$ nm) to continuously heat aerosol particles. After the aerosol particles absorb high energy laser energy quickly, the laser induces combustion instantaneously and emits incandescence. The concentration and mixed state of BC were measured with the scattering signal of aerosol particles and the incandescent light signal, respectively. The particle size range was about 70–500 nm. Ambient particulate matter components were measured online with a high-resolution time-of-flight aerosol mass spectrometer (HR-ToF-AMS, Aerodyne, USA). The HOA was resolved by the positive matrix factorization (PMF) analysis based on the high resolution mass spectral data of AMS;[28,29] it had the lowest oxygen-to-carbon ratio (O/C) of 0.14 and highest hydrocarbon-to-carbon ratio (H/C) of 1.56 among all factors, which is associated to the fresh emission from on road vehicles.

Results and discussion

To investigate the diurnal profile of particle number size distribution and black carbon number size distribution, the observation periods were divided into three categories. From an observational perspective, when NPF occurs, the time-series isocontour plots of particle number size distributions often exhibit a distinct banana-shaped characteristic. Therefore, when this phenomenon occurs on a given day,[30–32] the day is defined as an NPF-day, and the rest are defined as non-NPF days. When the ambient daily averaged $PM_{2.5}$ concentration exceeds 15 $\mu g\,m^{-3}$, it is called a haze day.[33] The diurnal variation in the particle number size distribution of total particles and BC during NPF, non-NPF and haze days are shown in Fig. 1. The particle size distribution shows distinct diurnal variations under different pollution events. Under NPF conditions, particles smaller than 100 nm in size are more abundant, which are found mainly at daytime (9:00–15:00), with their peak concentrations of up to 10^5 # cm^{-3}. The substantial formation of nanoparticles under NPF conditions is mainly due to the low condensation sink (CS) with an average value of 0.005 s^{-1}, which minimizes the coagulation effect of large particles on nanoparticles.[15,34] During the non-NPF and haze days, high particle concentration occurred in the evening period (18:00–21:00) and early morning hours (0:00–6:00), which can be attributed to a shallow boundary layer height and increased emission from motor vehicles given the large number of vehicles in Beijing. BC as well as NMPs, are typical particles emitted by on-road vehicles. The size distribution of BC is mainly concentrated around 100 nm, with high concentrations originating from evening rush hours until early morning, which is consistent with the distribution of total particle number size distributions.

To confirm the significant influence of vehicle emissions on nanoparticle formation rather than the development of boundary layer height, the daily variation in HOA divided by the mass concentration of BC was plotted in Fig. 2a, which removed

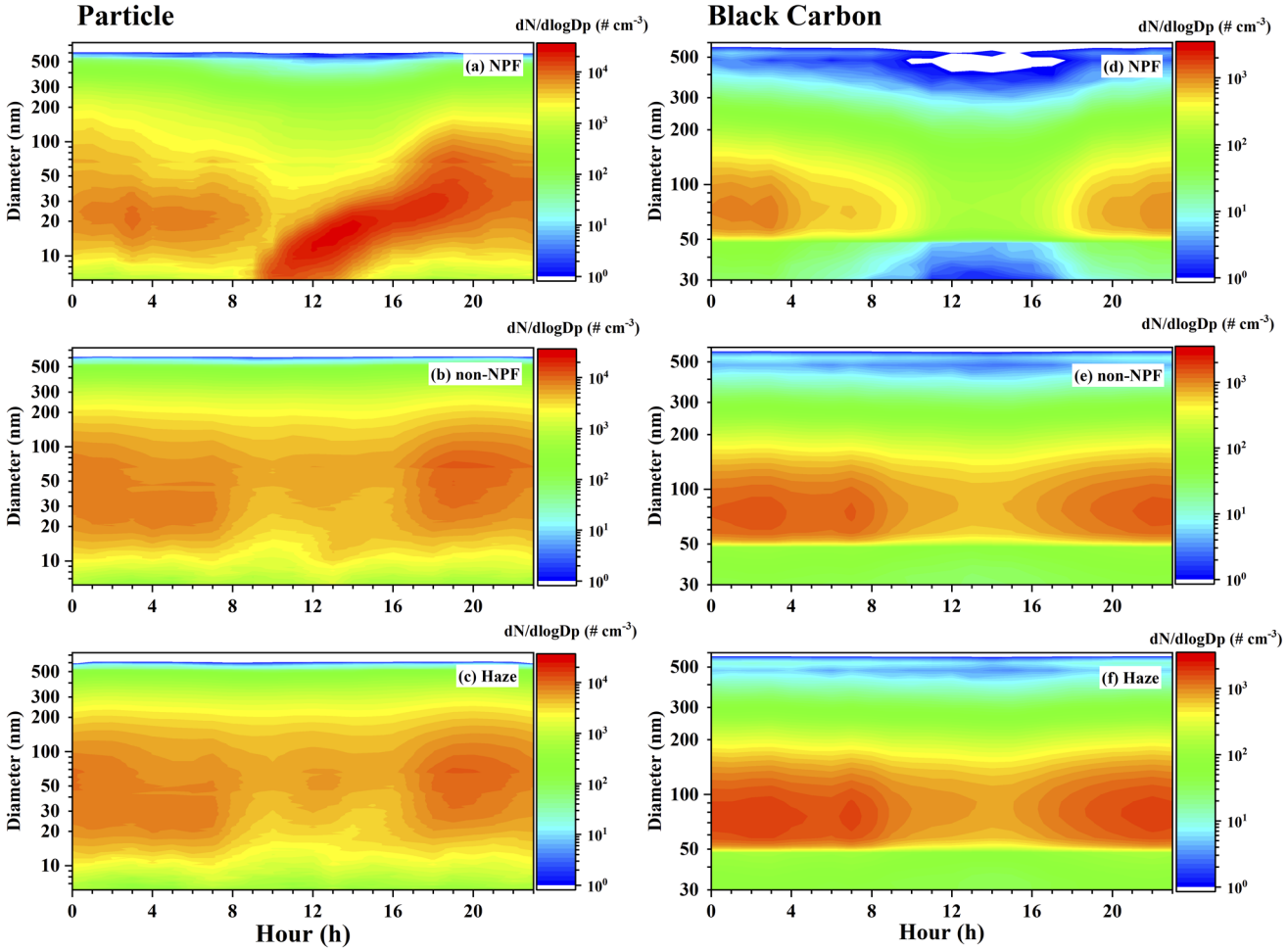

Fig. 1 Diurnal variation in total particle size distribution from 5 nm to 700 nm during (a) new particle formation day; (b) non-NPF day; and (c) haze day. Diurnal variation in black carbon number size distribution from 50–700 nm in the three conditions (d–f).

the boundary layer dilution effect. HOA and the particle size distribution pattern of BC are higher in the early morning and evening peak periods. The diurnal variation in Dp/Dc is presented in Fig. 2b, which is analyzed in conjunction with the particle size distribution of BC (Fig. 1d–f). Dp/Dc is low at night but increases during the daytime (07:00–15:00), which is probably due to the strong photochemical reactions and effects of the long-range transport process of the aged air mass.

To further show the influence of on-road vehicle emissions on the formation of NMPs, the correlation between NMPs and HOA is depicted in Fig. 3. We analyzed the relationship between the particle number concentration of NMP and HOA as well as the average concentration of NMP under different conditions and HOA. On NPF days, NMPs were negatively correlated with HOA, suggesting that NPF mainly occurred during the daytime when vehicle emissions were relatively low. However, the correlation between HOA and NMPs are positive during non-NPF and haze days, which suggests that motor vehicle emissions also make a direct contribution to NMPs.

From the above analysis, both NPF and on-road vehicle emissions contribute to the formation of NMPs in Beijing, but the exact contribution is not clear. Based on the Dp/Dc that characterizes the thickness of the BC coating, the air masses arriving at the observation site are classified into two categories. High values of Dp/Dc correspond to aged air masses, which come from long-range transport, while low values of Dp/Dc are fresh air masses from local NPF and direct emissions. Based on the literature, a Dp/Dc ratio of 1.5 is used as a threshold to distinguish between fresh local air masses and aged air masses from upwind regions.[35–37]

As shown in Fig. 4a–c, respectively, the NMP concentration varies remarkably with the Dp/Dc ratio during NPF, non-NPF and haze days. Using the threshold value of Dp/Dc as a reference, NMP concentrations were higher during NPF days, whereas they remained low during non-NPF and haze days. This indicates the rapid aging of BC during non-NPF and haze days due to the abundance of gas vapors and significant coagulation loss of NMPs by the high condensation sink.

Otherwise, within fresh local air masses, the contribution of direct motor vehicle emissions is relatively constant in different pollution scenarios, and the main contributor to NMPs is new particle formation. It was assumed that the NMPs observed in fresh air masses during non-NPF and haze days were mainly attributable to direct on-road vehicle emissions, whereas those

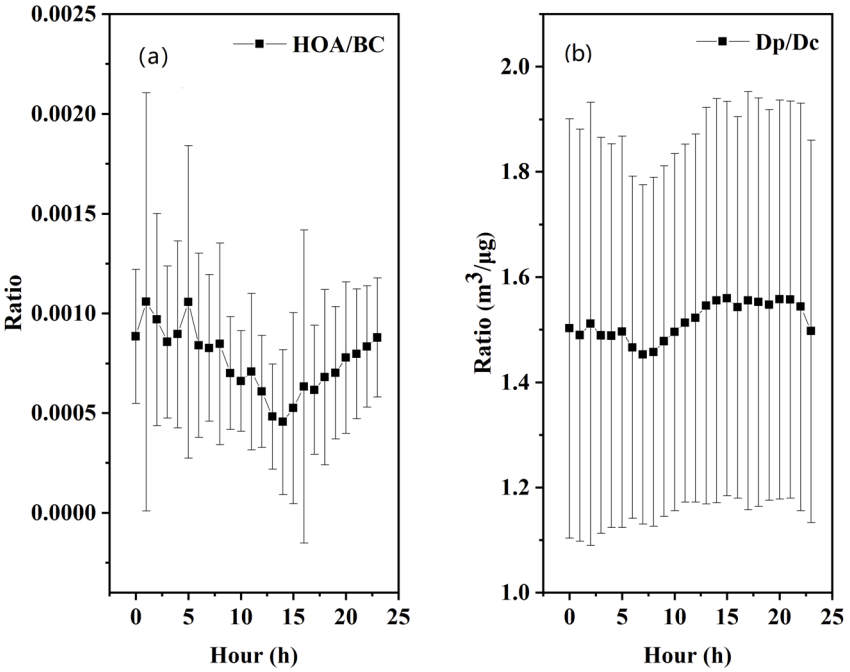

Fig. 2 Diurnal variations in (a) hydrocarbon organic aerosol (HOA) mass concentration resolved by PMF from the spectrum of organic aerosol, which removed the influence of boundary layer dilution effect and expressed as HOA/BC. (b) Ratio of the diameter of the whole particle (including coatings and BC core) to the BC core, defined as Dp/Dc; the squares represent the average values, and the bars represent standard deviation.

observed during NPF days were attributable to both new particle formation and vehicle emissions. A simple statistical result shows that the weighted average NMP concentration during NPF, non-NPF and haze days are 1704 # cm^{-3}, 554 # cm^{-3}, 180 # cm^{-3}, respectively. The contributions of NPF and motor vehicle emissions to the formation of NMPs are shown in Fig. 5; from 18:00 to 08:00, we consider the main source of NMP to be motor vehicle emissions, with an average concentration of 204 # cm^{-3}. From 09:00–17:00, we consider the main source of NMP to be NPF, with an average concentration of 1615 # cm^{-3}. Overall, the contribution of NPF to NMP formation is 89% and that of on-road vehicle emissions is 11% during NPF days based on their respective average concentrations (1615 and 204 # cm^{-3}) and a total concentration of 1819 # cm^{-3} for the daytime.

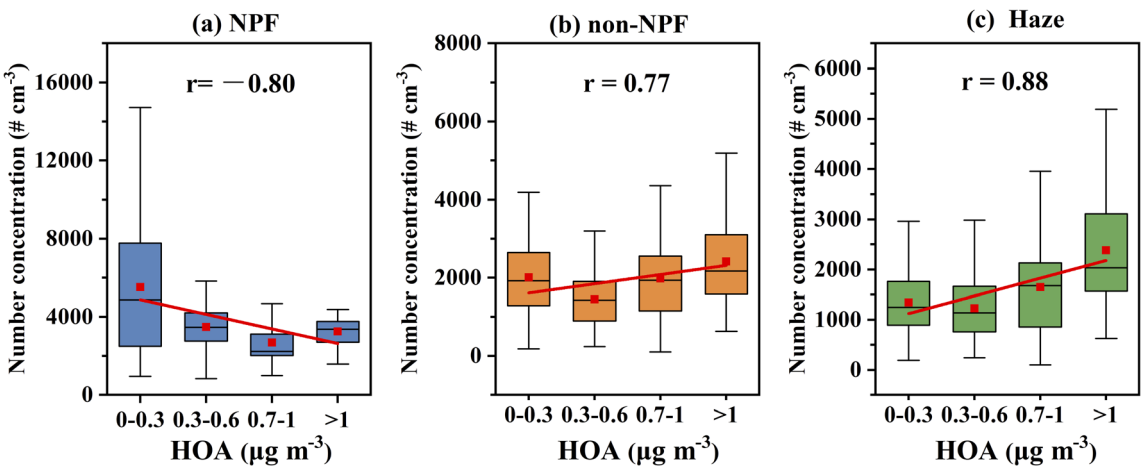

Fig. 3 Relationship between HOA mass concentrations and nucleation mode particle number concentration during (a) NPF day, (b) non-NPF day and (c) haze day. The *X*-axis of the figure is the mass concentration of HOA, and the left *Y*-axis is the total particle number concentration of nucleation mode particles. In the Box–whisker plot, the solid black line in the middle of the box represents the median of the data. The top and bottom of the box, respectively, are the upper quartile (Q3) and lower quartile (Q1) of the data. The top and bottom edges of the box are the maximum and minimum values of the particle number concentration, respectively. The points on the outside of the box are the outliers in the data. The colored solid lines are obtained from a linear fit of the average particle number concentration of particulate matter to HOA.

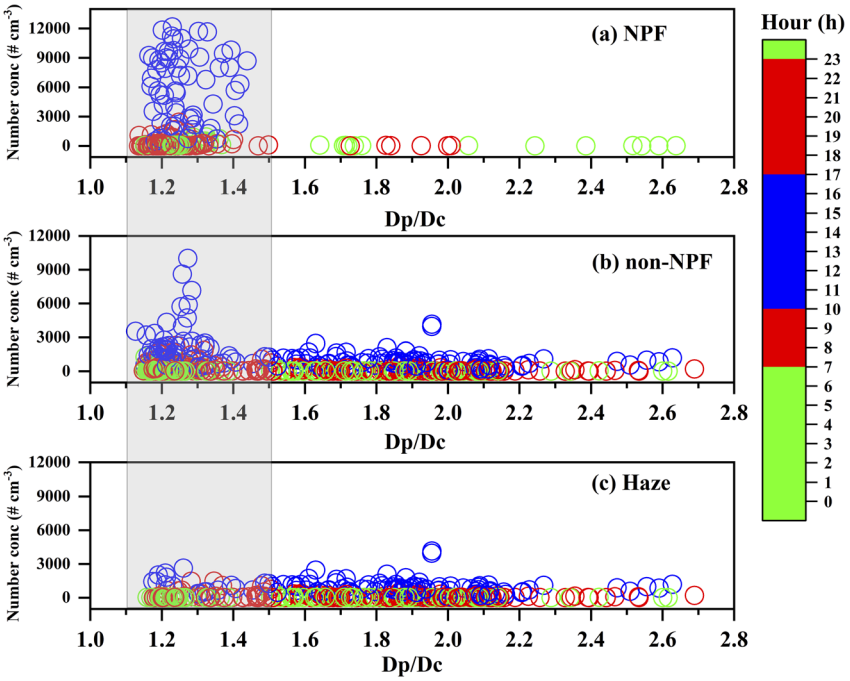

Fig. 4 Relationship between NMPs and Dp/Dc during (a) NPF (b) non-NPF and (c) haze days. The color bar represents the hour of the day, and the shadowed areas correspond to NMP concentrations with a Dp/Dc ratio of less than 1.5.

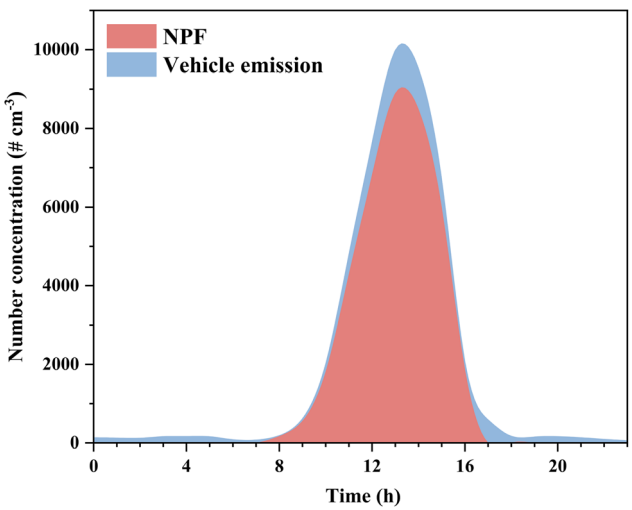

Fig. 5 Real-time curves of the contributions of NPF and motor vehicle emission to NMP formation on NPF days.

Conclusions

In this study, we applied a novel method of evaluating the BC coating thickness for analyzing the source of NMPs in the megacity Beijing. Using this method, the influence of long-range transported air masses could be reasonably excluded, as they were characterized by a larger coating-thickness-to-BC-core ratio. We identified local direct motor vehicle emissions and NPF as the main sources of NMP. Our results show that NPF has a major contribution to the formation of NMPs, and on-road vehicle emissions are a relatively constant source of NMPs. We suggest that more similar investigations should be conducted in other urban atmospheres for comparison studies on the contribution of NPF and direction emissions to NMP formation.

Author contributions

Y. W. designed the research. H. Z., Y. W., Q. L., J. L., T. C., P. Z., Q. M., and B. C. conducted the field campaign. H. Z., J. L. and Y. W. performed the experimental studies. H. Z., J. L. and Y. W. wrote the main manuscript with contribution from all coauthors.

Conflicts of interest

The authors declare no conflicts of interest.

Data availability

All the data used for plotting the figures in the main text are available upon request to the corresponding author.

Acknowledgements

This study was supported by the National Key Research and Development Program of China (2023YFC3711000) and the National Natural Science Foundation of China (42205098, 42405098 and 22188102).

References

1 M. Kulmala, V. M. Kerminen, T. Petaja, A. J. Ding and L. Wang, Atmospheric gas-to-particle conversion: why NPF events are observed in megacities?, *Faraday Discuss.*, 2017, **200**, 271–288.

2 M. Kulmala, J. Kontkanen, H. Junninen, K. Lehtipalo, H. E. Manninen, T. Nieminen, T. Petaja, M. Sipila, S. Schobesberger, P. Rantala, A. Franchin, T. Jokinen, E. Jarvinen, M. Aijala, J. Kangasluoma, J. Hakala, P. P. Aalto, P. Paasonen, J. Mikkila, J. Vanhanen, J. Aalto, H. Hakola, U. Makkonen, T. Ruuskanen, R. L. Mauldin III, J. Duplissy, H. Vehkamaki, J. Back, A. Kortelainen, I. Riipinen, T. Kurten, M. V. Johnston, J. N. Smith, M. Ehn, T. F. Mentel, K. E. Lehtinen, A. Laaksonen, V. M. Kerminen and D. R. Worsnop, Direct observations of atmospheric aerosol nucleation, *Science*, 2013, **339**(6122), 943–946.

3 T. Olenius, T. Yli-Juuti, J. Elm, J. Kontkanen and I. Riipinen, New Particle Formation and Growth. In *Physical Chemistry of Gas–Liquid Interfaces*, 2018, pp. 315–352.

4 J. Merikanto, D. V. Spracklen, G. W. Mann, S. J. Pickering and K. S. Carslaw, Impact of nucleation on global CCN, *Atmos. Chem. Phys.*, 2009, **9**(21), 8601–8616.

5 D. V. Spracklen, K. S. Carslaw, M. Kulmala, V.-M. Kerminen, S.-L. Sihto, I. Riipinen, J. Merikanto, G. W. Mann, M. P. Chipperfield, A. Wiedensohler, W. Birmili and H. Lihavainen, Contribution of particle formation to global cloud condensation nuclei concentrations, *Geophys. Res. Lett.*, 2008, **35**(6), L06808.

6 S. C. Anenberg, J. Miller, R. Minjares, L. Du, D. K. Henze, F. Lacey, C. S. Malley, L. Emberson, V. Franco, Z. Klimont and C. Heyes, Impacts and mitigation of excess diesel-related NOx emissions in 11 major vehicle markets, *Nature*, 2017, **545**(7655), 467–471.

7 J. Wang, Q. Wu, J. Liu, H. Yang, M. Yin, S. Chen, P. Guo, J. Ren, X. Luo, W. Linghu and Q. Huang, Vehicle emission and atmospheric pollution in China: problems, progress, and prospects, *PeerJ*, 2019, **7**, e6932.

8 T. Ronkko, H. Kuuluvainen, P. Karjalainen, J. Keskinen, R. Hillamo, J. V. Niemi, L. Pirjola, H. J. Timonen, S. Saarikoski, E. Saukko, A. Jarvinen, H. Silvennoinen, A. Rostedt, M. Olin, J. Yli-Ojanpera, P. Nousiainen, A. Kousa and M. Dal Maso, Traffic is a major source of atmospheric nanocluster aerosol, *Proc. Natl. Acad. Sci. U. S. A.*, 2017, **114**(29), 7549–7554.

9 J. Hofman, J. Staelens, R. Cordell, C. Stroobants, N. Zikova, S. M. L. Hama, K. P. Wyche, G. P. A. Kos, S. Van Der Zee, K. L. Smallbone, E. P. Weijers, P. S. Monks and E. Roekens, Ultrafine particles in four European urban environments: Results from a new continuous long-term monitoring network, *Atmos. Environ.*, 2016, **136**, 68–81.

10 L. Calderón-Garcidueñas and A. Ayala, Air Pollution, Ultrafine Particles, and Your Brain: Are Combustion Nanoparticle Emissions and Engineered Nanoparticles Causing Preventable Fatal Neurodegenerative Diseases and Common Neuropsychiatric Outcomes?, *Environ. Sci. Technol.*, 2022, **56**(11), 6847–6856.

11 W. Nie, A. Ding, T. Wang, V.-M. Kerminen, C. George, L. Xue, W. Wang, Q. Zhang, T. Petäjä, X. Qi, X. Gao, X. Wang, X. Yang, C. Fu and M. Kulmala, Polluted dust promotes new particle formation and growth, *Sci. Rep.*, 2014, **4**(1), 1–6.

12 T. Rönkkö, H. Kuuluvainen, P. Karjalainen, J. Keskinen, R. Hillamo, J. V. Niemi, L. Pirjola, H. J. Timonen, S. Saarikoski, E. Saukko, A. Järvinen, H. Silvennoinen, A. Rostedt, M. Olin, J. Yli-Ojanperä, P. Nousiainen, A. Kousa and M. Dal Maso, Traffic is a major source of atmospheric nanocluster aerosol, *Proc. Natl. Acad. Sci. U. S. A.*, 2017, **114**(29), 7549–7554.

13 L. Yao, O. Garmash, F. Bianchi, J. Zheng, C. Yan, J. Kontkanen, H. Junninen, S. B. Mazon, M. Ehn, P. Paasonen, M. Sipilä, M. Wang, X. Wang, S. Xiao, H. Chen, Y. Lu, B. Zhang, D. Wang, Q. Fu, F. Geng, L. Li, H. Wang, L. Qiao, X. Yang, J. Chen, V.-M. Kerminen, T. Petäjä, D. R. Worsnop, M. Kulmala and L. Wang, Atmospheric new particle formation from sulfuric acid and amines in a Chinese megacity, *Science*, 2018, **361**(6399), 278–281.

14 R. Cai, C. Yan, D. Yang, R. Yin, Y. Lu, C. Deng, Y. Fu, J. Ruan, X. Li, J. Kontkanen, Q. Zhang, J. Kangasluoma, Y. Ma, J. Hao, D. R. Worsnop, F. Bianchi, P. Paasonen, V.-M. Kerminen, Y. Liu, L. Wang, J. Zheng, M. Kulmala and J. Jiang, Sulfuric acid–amine nucleation in urban Beijing, *Atmos. Chem. Phys.*, 2021, **21**(4), 2457–2468.

15 Y. Wang, Y. Ma, C. Yan, L. Yao, R. Cai, S. Li, Z. Lin, X. Zhao, R. Yin, C. Deng, J. Kangasluoma, X. C. He, S. Hakala, X. Fan, S. Chen, Q. Ma, V. M. Kerminen, T. Petäjä, J. Xin, L. Wang, B. Liu, W. Wang, M. Ge, J. Jiang, Y. Liu, F. Bianchi, B. Chu, N. M. Donahue, S. T. Martin, H. He and M. Kulmala, Sulfur Dioxide Transported From the Residual Layer Drives Atmospheric Nucleation During Haze Periods in Beijing, *Geophys. Res. Lett.*, 2023, **50**(6), e2022GL100514.

16 L. Chen, X. Qi, G. Niu, Y. Li, C. Liu, S. Lai, Y. Liu, W. Nie, C. Yan, J. Wang, X. Chi, P. Paasonen, T. Hussein, K. Lehtipalo, V.-M. Kerminen, T. Petäjä, M. Kulmala and A. Ding, High Concentration of Atmospheric Sub-3 nm Particles in Polluted Environment of Eastern China: New Particle Formation and Traffic Emission, *J. Geophys. Res.: Atmos.*, 2023, **128**(22), e2023JD039669.

17 C. Yan, R. Yin, Y. Lu, L. Dada, D. Yang, Y. Fu, J. Kontkanen, C. Deng, O. Garmash, J. Ruan, R. Baalbaki, M. Schervish, R. Cai, M. Bloss, T. Chan, T. Chen, Q. Chen, X. Chen, Y. Chen, B. Chu, K. Dällenbach, B. Foreback, X. He, L. Heikkinen, T. Jokinen, H. Junninen, J. Kangasluoma, T. Kokkonen, M. Kurppa, K. Lehtipalo, H. Li, H. Li, X. Li, Y. Liu, Q. Ma, P. Paasonen, P. Rantala, R. E. Pileci, A. Rusanen, N. Sarnela, P. Simonen, S. Wang, W. Wang, Y. Wang, M. Xue, G. Yang, L. Yao, Y. Zhou, J. Kujansuu, T. Petäjä, W. Nie, Y. Ma, M. Ge, H. He, N. M. Donahue, D. R. Worsnop, K. Veli-Matti, L. Wang, Y. Liu, J. Zheng, M. Kulmala, J. Jiang and F. Bianchi, The Synergistic Role of Sulfuric Acid, Bases, and Oxidized Organics Governing

New-Particle Formation in Beijing, *Geophys. Res. Lett.*, 2021, **48**(7), e2020GL091944.

18 Y. Wang, P. Clusius, C. Yan, K. Dällenbach, R. Yin, M. Wang, X.-C. He, B. Chu, Y. Lu, L. Dada, J. Kangasluoma, P. Rantala, C. Deng, Z. Lin, W. Wang, L. Yao, X. Fan, W. Du, J. Cai, L. Heikkinen, Y. J. Tham, Q. Zha, Z. Ling, H. Junninen, T. Petäjä, M. Ge, Y. Wang, H. He, D. R. Worsnop, V.-M. Kerminen, F. Bianchi, L. Wang, J. Jiang, Y. Liu, M. Boy, M. Ehn, N. M. Donahue and M. Kulmala, Molecular Composition of Oxygenated Organic Molecules and Their Contributions to Organic Aerosol in Beijing, *Environ. Sci. Technol.*, 2022, **56**(2), 770–778.

19 M. Kulmala, L. Dada, K. R. Daellenbach, C. Yan, D. Stolzenburg, J. Kontkanen, E. Ezhova, S. Hakala, S. Tuovinen, T. V. Kokkonen, M. Kurppa, R. Cai, Y. Zhou, R. Yin, R. Baalbaki, T. Chan, B. Chu, C. Deng, Y. Fu, M. Ge, H. He, L. Heikkinen, H. Junninen, Y. Liu, Y. Lu, W. Nie, A. Rusanen, V. Vakkari, Y. Wang, G. Yang, L. Yao, J. Zheng, J. Kujansuu, J. Kangasluoma, T. Petaja, P. Paasonen, L. Jarvi, D. Worsnop, A. Ding, Y. Liu, L. Wang, J. Jiang, F. Bianchi and V. M. Kerminen, Is reducing new particle formation a plausible solution to mitigate particulate air pollution in Beijing and other Chinese megacities?, *Faraday Discuss.*, 2021, **226**, 334–347.

20 M. Kulmala and V.-M. Kerminen, On the formation and growth of atmospheric nanoparticles, *Atmos. Res.*, 2008, **90**(2–4), 132–150.

21 Q. Zhang, J. L. Jimenez, M. R. Canagaratna, I. M. Ulbrich, N. L. Ng, D. R. Worsnop and Y. Sun, Understanding atmospheric organic aerosols via factor analysis of aerosol mass spectrometry: a review, *Anal. Bioanal. Chem.*, 2011, **401**(10), 3045–3067.

22 T. W. Chan, E. Meloche, J. Kubsh and R. Brezny, Black Carbon Emissions in Gasoline Exhaust and a Reduction Alternative with a Gasoline Particulate Filter, *Environ. Sci. Technol.*, 2014, **48**(10), 6027–6034.

23 M. Zavala, L. T. Molina, T. I. Yacovitch, E. C. Fortner, J. R. Roscioli, C. Floerchinger, S. C. Herndon, C. E. Kolb, W. B. Knighton, V. H. Paramo, S. Zirath, J. A. Mejía and A. Jazcilevich, Emission factors of black carbon and co-pollutants from diesel vehicles in Mexico City, *Atmos. Chem. Phys.*, 2017, **17**(24), 15293–15305.

24 E. Weingartner, H. Burtscher and U. Baltensperger, Hygroscopic properties of carbon and diesel soot particles, *Atmos. Environ.*, 1997, **31**(15), 2311–2327.

25 G. R. McMeeking, T. Hamburger, D. Liu, M. Flynn, W. T. Morgan, M. Northway, E. J. Highwood, R. Krejci, J. D. Allan, A. Minikin and H. Coe, Black carbon measurements in the boundary layer over western and northern Europe, *Atmos. Chem. Phys.*, 2010, **10**(19), 9393–9414.

26 J. P. Schwarz, R. S. Gao, D. W. Fahey, D. S. Thomson, L. A. Watts, J. C. Wilson, J. M. Reeves, M. Darbeheshti, D. G. Baumgardner, G. L. Kok, S. H. Chung, M. Schulz, J. Hendricks, A. Lauer, B. Kärcher, J. G. Slowik, K. H. Rosenlof, T. L. Thompson, A. O. Langford, M. Loewenstein and K. C. Aikin, Single-particle measurements of midlatitude black carbon and light-scattering aerosols from the boundary layer to the lower stratosphere, *J. Geophys. Res.*, 2006, **111**(D16), D16207.

27 N. Moteki and Y. Kondo, Effects of Mixing State on Black Carbon Measurements by Laser-Induced Incandescence, *Aerosol Sci. Technol.*, 2007, **41**(4), 398–417.

28 P. Paatero and U. Tapper, Positive matrix factorization: A non-negative factor model with optimal utilization of error estimates of data values, *Environmetrics*, 1994, **5**(2), 111–126.

29 I. M. Ulbrich, M. R. Canagaratna, Q. Zhang, D. R. Worsnop and J. L. Jimenez, Interpretation of organic components from Positive Matrix Factorization of aerosol mass spectrometric data, *Atmos. Chem. Phys.*, 2009, **9**(9), 2891–2918.

30 D. Shang, M. Hu, L. Tang, X. Fang, Y. Liu, Y. Wu, Z. Du, X. Cai, Z. Wu, S. Lou, M. Hallquist, S. Guo and Y. Zhang, Significant effects of transport on nanoparticles during new particle formation events in the atmosphere of Beijing, *Particuology*, 2023, **80**, 1–10.

31 M. Dal Maso, M. Kulmala, I. Riipinen, R. Wagner, T. Hussein, P. P. Aalto and K. E. Lehtinen, Formation and growth of fresh atmospheric aerosols: eight years of aerosol size distribution data from SMEAR II, Hyytiälä, Finland, *Boreal Environ. Res.*, 2005, **10**(5), 323.

32 V.-M. Kerminen, X. Chen, V. Vakkari, T. Petäjä, M. Kulmala and F. Bianchi, Atmospheric new particle formation and growth: review of field observations, *Environ. Res. Lett.*, 2018, **13**(10), 103003.

33 A. Goshua, C. A. Akdis and K. C. Nadeau, World Health Organization global air quality guideline recommendations: Executive summary, *Allergy*, 2022, **77**(7), 1955–1960.

34 R. Cai, R. Yin, C. Yan, D. Yang, C. Deng, L. Dada, J. Kangasluoma, J. Kontkanen, R. Halonen, Y. Ma, X. Zhang, P. Paasonen, T. Petäjä, V.-M. Kerminen, Y. Liu, F. Bianchi, J. Zheng, L. Wang, J. Hao, J. N. Smith, N. M. Donahue, M. Kulmala, D. R. Worsnop and J. Jiang, The missing base molecules in atmospheric acid–base nucleation, *Natl. Sci. Rev.*, 2022, **9**(10), nwac137.

35 Y. Zhang, M. Li, Y. Cheng, G. Geng, C. Hong, H. Li, X. Li, D. Tong, N. Wu, X. Zhang, B. Zheng, Y. Zheng, Y. Bo, H. Su and Q. Zhang, Modeling the aging process of black carbon during atmospheric transport using a new approach: a case study in Beijing, *Atmos. Chem. Phys.*, 2019, **19**(14), 9663–9680.

36 D. Liu, R. Joshi, J. Wang, C. Yu, J. D. Allan, H. Coe, M. J. Flynn, C. Xie, J. Lee, F. Squires, S. Kotthaus, S. Grimmond, X. Ge, Y. Sun and P. Fu, Contrasting physical properties of black carbon in urban Beijing between winter and summer, *Atmos. Chem. Phys.*, 2019, **19**(10), 6749–6769.

37 Y. Zhang, Q. Zhang, Y. Cheng, H. Su, H. Li, M. Li, X. Zhang, A. Ding and K. He, Amplification of light absorption of black carbon associated with air pollution, *Atmos. Chem. Phys.*, 2018, **18**(13), 9879–9896.